ELSEVIER

International Journal of Mass Spectrometry 189 (1999) 47–51

International Journal of Mass Spectrometry

A modular ion beam deflector

David A. Dahl*, Anthony D. Appelhans, Michael B. Ward

Idaho National Engineering and Environmental Laboratory, Idaho Falls, ID 83415, USA

Received 23 December 1998; accepted 18 March 1999

Abstract

A modular electrostatic ion beam deflector has been designed and tested that provides well-isolated *xy* deflection with minimal beam distortion using a single supply voltage per deflector stage. The convenient stacked electrode design of these deflectors facilitates precise assembly while providing good field termination and isolation characteristics. (Int J Mass Spectrom 189 (1999) 47–51) © 1999 Elsevier Science B.V.

Keywords: Ion optics; Secondary ion mass spectrometry; Ion trap

1. Introduction

Adjustable electrostatic ion beam deflectors are frequently employed in many instruments and experimental setups. They support functions varying from beam alignment to scanning. In its simplest embodiment, an electrostatic deflector is merely two parallel plates of differing electrostatic potential [1]. This apparent simplicity invites the casual inclusion of two (1D) or four (2D) plate deflectors in many experimental instruments. Although these simple deflector designs do deflect the ion beams, they typically add undesirable beam distortion effects. The ion beam deflector design discussed below was developed to provide convenient 1D and 2D ion beam deflectors that would deflect ion beams with minimal distortion and be modular enough to be easily employed in experimental instrumentation.

2. Discussion

Ideally, an ion beam deflector should add a transverse velocity component to each ion passing through it that is some fixed percentage of the ion's axial velocity component through the deflector. In principle, a linear electrostatic gradient that is transverse to the ion beam can provide the desired deflection characteristics:

$$\frac{V_T}{V_A} = \frac{EL}{2ke} \tag{1}$$

In Eq. (1) above, the ratio of an ion's transverse deflection velocity to its axial velocity through the deflector is equal to the electrostatic field gradient E (eV/m) multiplied by the axial length of the transverse electrostatic field L (m) divided by twice the ion's kinetic energy per unit charge ke (eV). This equation was derived assuming simple transverse electrostatic deflection and it ignores the acceleration effects of the transition fields that the ions encounter when entering

* Corresponding author.

1387-3806/99/$20.00 © 1999 Elsevier Science B.V. All rights reserved
PII S1387-3806(99)00051-2

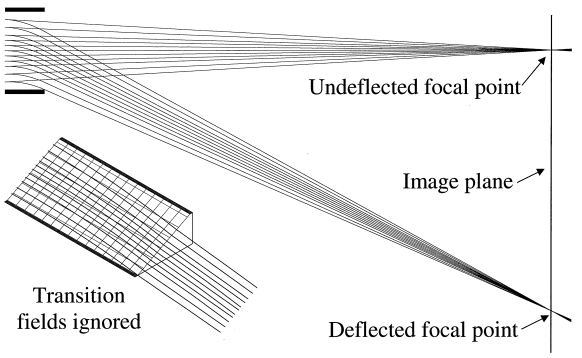

Fig. 1. Ion trajectories for a focused ion beam passing through an ideal electrostatic deflector with and without deflection, and the potential energy surface (inset) of the field within the deflector. Note that the field outside of the deflector has been forced to zero; thus there is no axial acceleration or deceleration as the ions enter or leave the deflector.

and leaving the deflector. A SIMION [2] simulation that also ignores any entry and exit field effects demonstrates the good deflection of a focusing ion beam provided in principle by a linear transverse electrostatic field (shown in Fig. 1). However, when the effects of the entrance and exit fields are included in an "extreme" example that maximizes their adverse impacts (shown in Fig. 2) a considerable amount of beam distortion results with the focus point shifting back toward the deflector. The potential energy surface shown in Fig. 2 serves to illustrate why this

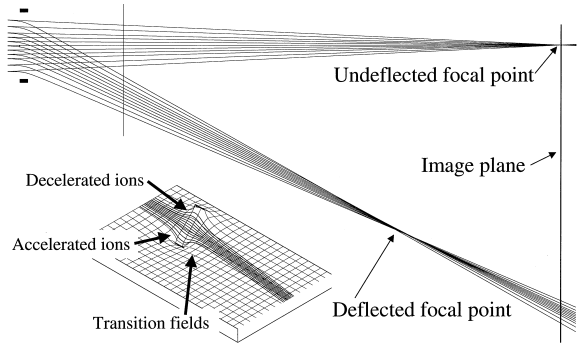

Fig. 2. Ion trajectories for a focused ion beam passing through a nonideal electrostatic deflector with and without deflection, and the potential energy surface (inset) of the field within and around the deflector. Note that the transition fields now result in axial acceleration or deceleration of the ions as they enter and leave the deflector region.

occurs. Ignoring any refractive effects of the transition fields, most of the beam distortion comes from the entry transition field that differentially changes the kinetic energy of each ion to match the potential at its point of entry in the transverse deflection field. Thus individual ions in a nonzero diameter ion beam will be differentially accelerated or decelerated according to their transverse location within the beam at point of entry into the deflector fields. Decelerated ions go slower, taking longer to traverse the deflector, and therefore gain higher transverse velocity components. Conversely, accelerated ions spend less time in the deflection region and thus gain relatively lower transverse velocity components. These differences in the transverse velocity between ions lead directly to the inward shift of the focus point and to the consequential beam distortion as can be seen in Fig. 2.

The key to reducing this type of deflector distortion is to reduce the induced differences in transverse ion velocities. The derived Eq. (2) gives the fractional change in transverse velocity ($\Delta V_T/V_{T0}$) of an ion offset a distance of r from an ion located on the beam axis in a transverse electrostatic field of E resulting in a change in ion kinetic energy of Δke relative to the beam axis ion. The velocity of the beam axis ion is V_{T0}, and its kinetic energy in the traverse deflection field is ke_0

$$\frac{\Delta V_T}{V_{T0}} = \frac{1}{\sqrt{1+\dfrac{\Delta ke}{ke_0}}} - 1 = \frac{1}{\sqrt{1+\dfrac{Er}{ke_0}}} - 1 \qquad (2)$$

$$\frac{\Delta V_T}{V_{T0}} \approx -\frac{1}{2}\frac{\Delta ke}{ke_0} = -\frac{1}{2}\frac{Er}{ke_0} \qquad (3)$$

A simplified approximation of Eq. (2) given by Eq. (3) provides a good estimate of the effect for fractional differences in ion kinetic energy ($\Delta ke/ke_0$) of 10% or less. These equations demonstrate that deflection induced distortions reduce as the fractional kinetic energy differences between ions within the deflection field are reduced. Assuming that the beam width r must remain unchanged, the easiest way to reduce the induced fractional kinetic energy differences is to lower the transverse electrostatic field

gradient (E) of the deflector. However, if the transverse electrostatic field gradients are reduced, the deflector length must be increased to retain the same beam deflection (V_T/V_A). Thus the first step to minimize distortion is to lengthen the deflector.

Additionally, precautions should be taken to insure that the electrostatic field between the deflector plates is highly linear. The primary problem is penetration of external fields into the region between the plates. The most effective way to minimize external field penetration is to maximize the deflectors' length to gap ratio. As a rule of thumb external field penetration is attenuated an order of magnitude for each 0.75 of a gap distance (planar symmetry assumed). For example, at a depth of 2.25 times the gap between the deflection plates an external field would be attenuated by a factor of 1000. Deflector length to gap ratios of 4.0 or above have proven quite satisfactory.

Two other issues also deserve consideration. First, field termination electrodes are desirable at the entrance and exit of a deflection stage to isolate the deflection stage from upstream and downstream fields and to provide well controlled deflector field termination (recommended depth to gap ratio ≥ 2). Second, the field termination electrodes and the deflection electrodes should have strong planar symmetry (fields invariant for z direction movements) to reduce possible xy deflection interactions when pairs of crossed deflector stages are used to obtain x and y deflection. Fig. 3 illustrates a simple pair of crossed deflectors embodying these principles, and the potential energy surface within a deflection stage to illustrate the role of the field termination electrodes.

SIMION simulations of the deflectors shown in Fig. 3 indicate excellent xy deflection interaction isolation, and relatively low beam imaging distortion. The beam's undeflected point image (0 microns in diameter—has perfect focus) distorts to a 15 micron radius of confusion when the beam is deflected 5 mm off axis. These simulation results are for a 4 mm diameter beam that focuses 275 mm downstream from the entrance of the first deflector. This assumes a gap between deflector plates of 6 mm and a total length of 45 mm for each deflector stage. Field termination electrodes have a length to gap ratio of 2, and the deflector electrodes have a length to gap ratio of 4.

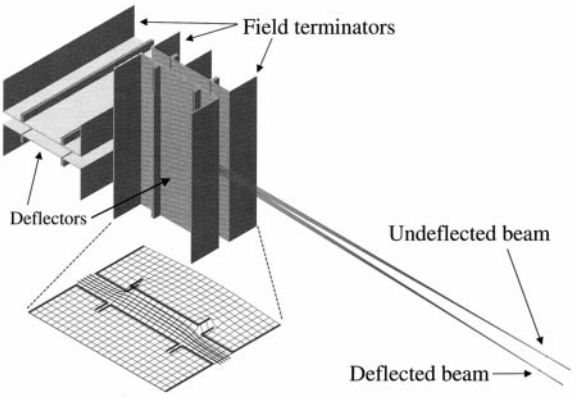

Fig. 3. A conceptual dual stage deflector with field terminators and the potential energy surface of one stage, along with deflected and undeflected ion trajectories of a focused ion beam.

3. Results and conclusions

These principles were used to design the modular deflector shown in Fig. 4. The deflector is assembled by stacking the various deflector electrodes onto a four rod assembly using precision ceramic insulators (Kimball Physics, Wilton, NH) to separate, align, and

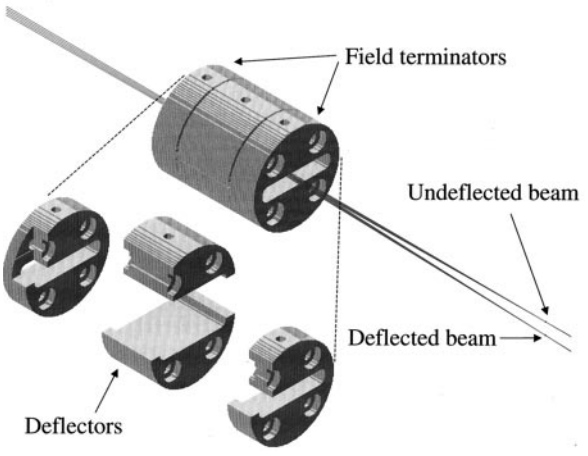

Fig. 4. SIMION model of a single stage of the modular deflector; the parts are interchangeable and designed to be stacked for multiple axis deflection.

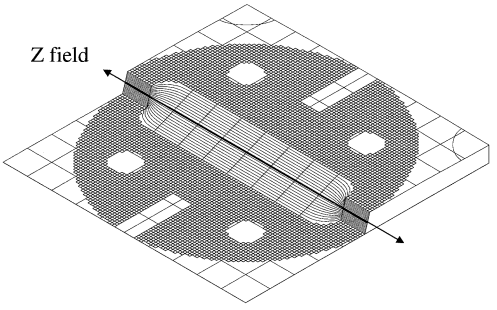

Fig. 5. Potential energy surface within a single stage of the deflector; note the uniformity and linearity of the field gradient and the symmetrical termination of the field in the *Z* direction.

electrically isolate the electrodes. The field termination electrodes have a length to gap ratio of approximately 2. The length to gap ratio of the deflection electrodes is approximately 4. The *z* length (edge to center) to gap ratio is approximately 2 for deflection electrodes and field termination electrodes. Note that the deflection electrodes use a centered narrow gap at their *z* field limits to help insure symmetrical *z* field termination. The potential energy surface shown in Fig. 5 illustrates the uniform field gradients in the beam region between these electrodes and the symmetrical *z* field termination in the narrow gap region.

Fig. 6. Photograph of the as-built dual stage deflector (top) and a set of components for a single stage.

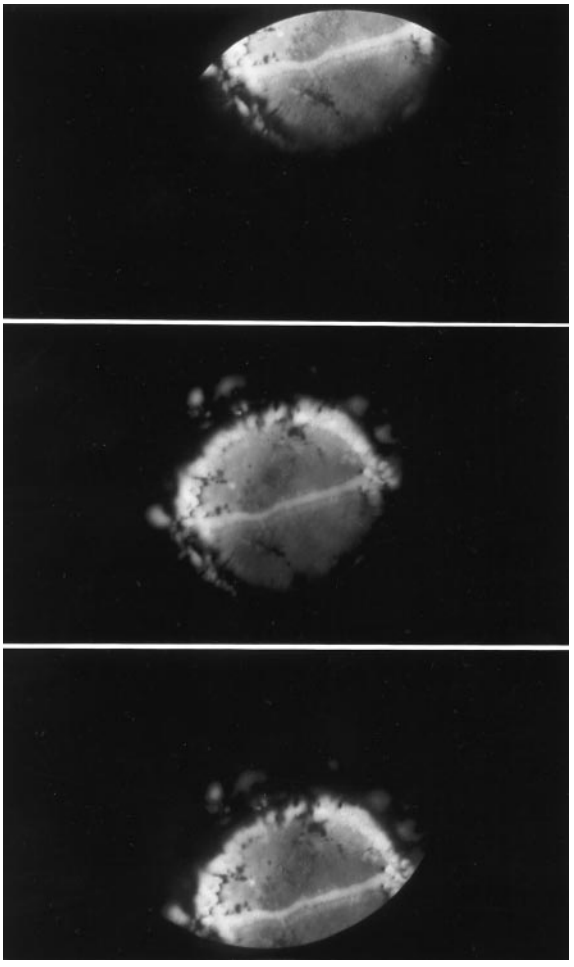

Fig. 7. Composite photograph of the image of an ion source projected onto an MCP detector. The center image was undeflected; the top and bottom images were deflected to the limits of the detector. The horizontal line resulted from a scratch placed on the face of the ion emitter for reference purposes.

Fig. 6 is a composite photograph of a two deflector stack used for *xy* deflection of the primary beam from our univoltage ion gun [3] with a collection of component electrodes displayed below. These deflectors have proven very satisfactory for deflecting 2 mm primary ion beams without noticeable distortion. Moreover, the relatively low deflection gradients involved permit the use of single supply voltage deflection (by grounding the opposite deflection electrode)

without incurring a noticeable increase in distortion. Fig. 7 illustrates the deflection of a magnified image of a perrhenate ion beam source that has been projected by the ion gun through an *xy* stack of modular deflectors onto a multichannel plate imaging detector (MCP) approximately 350 mm downstream from the source. The 1 mm source's image (with a horizontal scratch across it to aid in identification) is magnified to approximately 10 mm in diameter and the upper and lower image deflections are MCP size limited. There is no noticeable distortion of the source image even for these relatively large deflections.

XY stacks of these modular deflectors have been incorporated into many of our group's ion trap and quadrupole secondary ionization mass spectrometry instruments for deflecting primary ion beams. SIMION geometry files and engineering drawings of these deflectors are available upon request.

References

[1] A. Benninghoven, R.G. Rudenauer, H.W. Werner, in Secondary Ion Mass Spectrometry Basic Concepts, Instrumental Aspects, Applications and Trends, Wiley, New York, 1987, p. 338.
[2] D.A. Dahl, SIMION 3D Version 6.0 User's Manual, INEL-95/0403 (1995).
[3] D.A. Dahl, A.D. Appelhans, M.B. Ward, Int. J. Mass Spectrom. 189 (1999) 39–46.